ONBOARD SCIENCE PRODUCT GENERATION ON THE EARTH OBSERVING ONE MISSION AND BEYOND

Steve Chien[(1)], Daniel Tran[(1)], Steve Schaffer[(1)], Gregg Rabideau[(1)], Ashley Gerard Davies[(1)], Thomas Doggett[(2)], Ronald Greeley[(2)], Felipe Ip[(3)], Victor Baker[(3)], Joshua Doubleday[(1)], Rebecca Castano[(1)], Dorothy Silverman[(1)], Daniel Mandl[(4)], Stuart Frye[(4)], Lawrence Ong[(4)], Petya Campbell[(4)], Bogdan Oaida[(1)]

[(1)]Jet Propulsion Laboratory, California Institute of Technology, 4800 Oak Grove Dr, Pasadena, CA 91109-8099, USA
[(2)]Arizona State University, Phoenix, AZ 85069-7100, USA
[(3)]University of Arizona, Tucson AZ 85721, USA
[(4)]Goddard Space Flight Center, Greenbelt, MD 20771, USA

ABSTRACT

Remote-sensed hyperspectral data represents significant challenges in downlink due to its large data volumes. This paper describes work developing and validating onboard processing of hyperspectral data products to (a) reduce data downlink volumes and (b) decrease latency to provide key data products (often by enabling use of lower data rate communications systems). We describe efforts to develop onboard processing to study volcanoes, floods, and cryosphere, using the Hyperion hyperspectral imager and onboard processing for the Earth Observing One (EO-1) mission as well as preliminary work targeting the Hyperspectral and Thermal Infrared Imager on the HyspIRI mission. ·

1. INTRODUCTION

We describe onboard processing algorithms for volcano, flood, and cryosphere analysis deployed onboard the Earth Observing One (EO-1) spacecraft and applied to Hyperion hyperspectral data. We also describe ongoing work to develop oceanographic applications for EO-1 as well as follow-on work targeting onboard processing for the HyspIRI mission. In each of these cases we describe the science processing steps as well as the runtime benchmarks for a range of flight processors.

The motivation for onboard processing is multifold. First, many space missions are downlink limited. Onboard processing can dramatically reduce the amount of data that needs to be returned. Second, onboard processing can enable more rapid data production. By processing the data onboard and reducing the data volume it is possible to downlink alerts or summary products via lower data rate engineering downlink – resulting in more rapid notification (an example of this is the Direct Broadcast system [Directbroadcast]). Third, onboard processing can enable onboard response providing more rapid response to science events. For example, EO-1 onboard science analysis can drive retasking the spacecraft - enabling response to science events within hours compared to routine ground-in-the-loop data processing and response of one week or rush ground response of several days.

· Correspondence author: steve.chien@jpl.nasa.gov
Portions of this work were performed by the Jet Propulsion Laboratory, California Institute of Technology, under contract with the National Aeronautics and Space Administration.

Proc. 'IJCAI–09 Workshop on Artificial Intelligence in Space', Pasadena, California, US 17–18 July 2009 (ESA SP-673, September 2009)

2. THE EARTH OBSERVING ONE MISSION AND THE AUTONOMOUS SCIENCECRAFT

EO-1 [Ungar et al. 2003] was launched in November 2000 into a 705-km circular orbit with an inclination of 98.7 degrees. This orbit affords global coverage, with approximate ground-repeat tracks every 16 days. EO-1 is a pointable spacecraft. Observations can be nadir, one path to the east or west, and two paths to the east or west. A target may therefore be imaged up to 10 times in any 16-day period, with five day and five night observations. For polar targets, where orbital paths converge, imaging up to five paths away from the nadir is theoretically possible.

On board EO-1 are three instruments: the Advanced Land Imager (ALI), the LEISA Atmospheric Corrector (LAC) and the Hyperion imaging spectrometer. ASE uses data from the Hyperion instrument although an effort is underway to enable onboard access to ALI data.

The Hyperion imaging spectrometer is a hyperspectral imager with 220 discrete bands covering a wavelength range of 0.4–2.5 μm. This spectral range makes Hyperion an excellent instrument for tracking many science phenomena that can be distinguished with these spectra. Hyperion has a spatial resolution of 30 m/pixel. A typical Hyperion observation is 7.7 km (256 pixels) wide by 95km (3176 pixels) long.

The Autonomous Sciencecraft Experiment (ASE) [Chien et al. 2005] is flight software that has been the primary means of operating the EO-1 mission since 2004. ASE has science processing, mission planning, and onboard execution components. The science processing component enables onboard analysis of Hyperion imagery to develop smaller products for rapid downlink, downlink of alerts, and to drive onboard decision-making. The onboard mission planning component enables EO-1 to change future observations based on detected events. The onboard execution component executes the mission plans and enables the overall system to be robust to run-time variances.

The ASE software has been operating the EO-1 spacecraft since 2004 and has successfully acquired over 20,000 images under software control. Further information on ASE can be found at ase.jpl.nasa.gov and [Chien et al. 2005]. This next section of this paper focuses on the onboard science element of ASE, specifically the onboard science element that processes Hyperion hyperspectral data onboard EO-1.

3. ONBOARD PROCESSING OF HYPERSPECTRAL HYPERION DATA ON EO-1

For the period 2005-2009 the ASE software performed onboard processing of three (3) event types: thermal detection and summarization to enable volcano science; flood classification of surface water to enable flood science; and snow water ice land (SWIL) classification to enable cryosphere science. The onboard science algorithm can extract 12 selectable bands of the 220 Hyperion bands for a patch of 256 wide (across track) by 1024 long (along track) pixels. In the following sections we describe these hyperspectral data analysis algorithms in greater detail.

3.1. Thermal Classification and Summarization

EO-1 is flying an onboard thermal detection and summarization algorithm [Davies et al. 2006]. This algorithm uses the infra-red bands of the Hyperion instrument to evaluate images for very hot (over 400 Kelvin) signatures. The thermal processing algorithms use a spectral gradient measure G = (2.28 μm - 1.65 μm)/(2.28 – 1.65) as well as a number of other thermally sensitive bands as shown below.

Description	Measure
H1: Hot radiance minimum and pixel not noisy	0.625 < 1.65 μm, 2.25 μm, & 2.28 μm < 750

H2: Min. slope for trigger?	Slope G > 0.13558 G=1.4 for DNs
H3/E3: No 2.28μm spike	(2.28μm+1.65μm)/2< 2.25μm*1.2
E1: Extreme radiance min.?	0.625 < 1.25 μm, 1.65 μm, & 2.28 μm < 750
E2: Spectrum shape	2.28 μm > 1.65 μm/2

The onboard thermal classification algorithm finds all pixels matching conditions H1, H2, & H3 listed above and labels them as "HOT". All remaining pixels that satisfy conditions E1, E2, and E3 are labeled as "EXTREME". The thermal algorithm downlinks a map of the hot and extreme pixels as well as the extracted 12 spectral bands of the hot and extreme pixels (of requested). Because the data allocation for the summary algorithms is limited if there are too many hot and extreme pixels only the first N will be downlinked. Figure 1 shows sample thermal products.

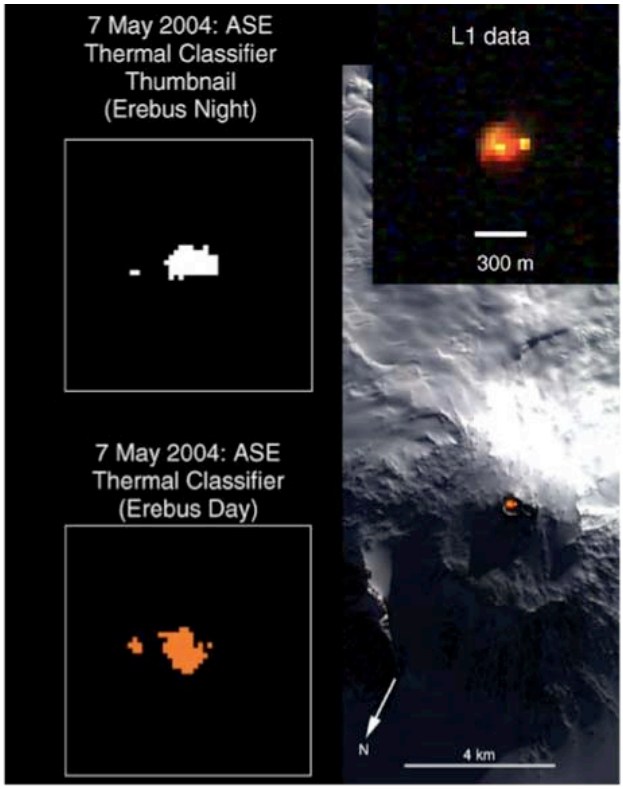

Figure 1: Hot and extreme pixel classification maps as well as Level One full data for EO-1/ASE trigger and autonomous response data acquired of the Mount Erebus volcano 7th May 2004 on two overflights. Figure courtesy [Davies et al. 2006].

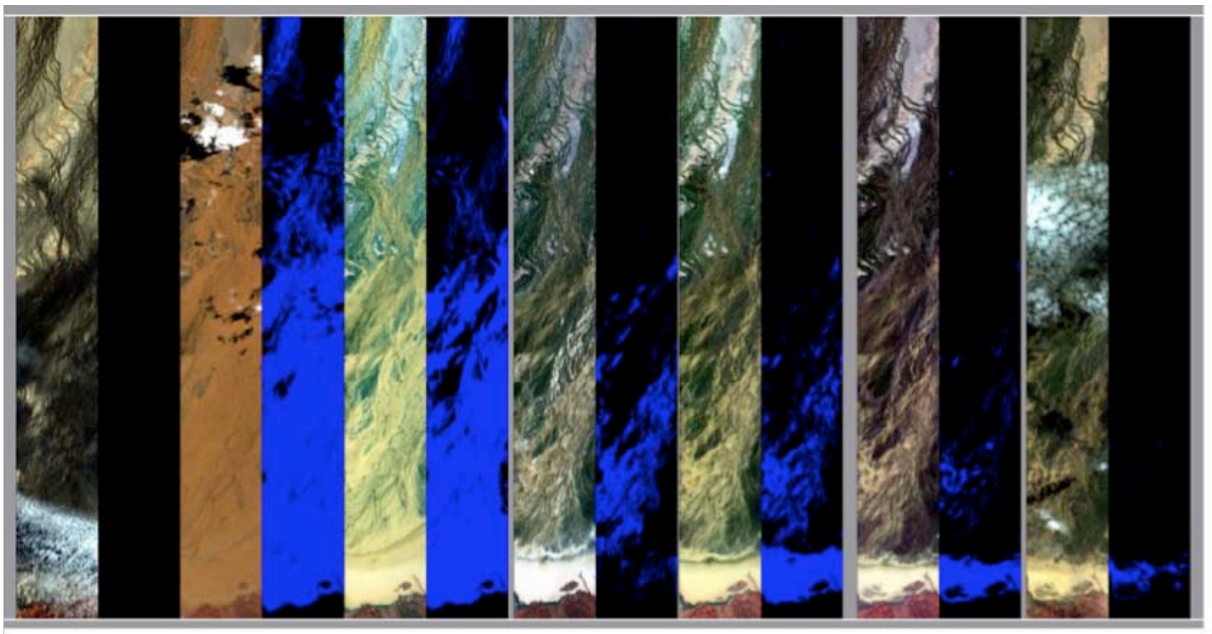

Figure 2: Diamantina flooding sequence. False color and classified scenes of prime sites (256×1024 pixels/7.7km×30km center subset of a Hyperion scene) along the Diamantina River, Australia (1/5/04, 1/30/04, 2/6/04, 2/13/04, 2/15,04, 2/22/04 and 2/29/04). This figure demonstrates the EO-1's 16-day-repeat cycle is sufficient to capture the onset and retreat of a flood event such as this one. Figure courtesy [Ip et al. 2006]

Description of cryosphere classifier steps in ASE release 3

Step	Algorithm	Classification	Notes
1	If $\rho_{0.66}/\rho_{0.86}>2.23$	Water	Inverse of the standard ratio vegetation index (Tucker, 1979)
2	$\rho_{0.56}/\rho_{0.86}>3.83$	Water	
3	$\rho_{0.56}/\rho_{0.86}<0.8$	Land	
4	$L_{1.65}>62.5$ or $L_{1.65}<0$	Unclassified	Filter for instrument noise, patched in ASE Release 3
5	NDSI<0.176	Unclassified	Cloud not picked up by Griffin et al. (2003), and shadow
6	$\rho_{0.56}/\rho_{0.66}<0.91$	Unclassified	Playa and other bright land lacking vegetation
7	NDSI>0.56 and $\rho_{0.56}/\rho_{0.66}<1.11$		
7a	$\rho_{0.56}/\rho_{0.66}<1$	Snow	
7b	$\rho_{0.86}/\rho_{1.65}>16$	Unclassified	Cloud not picked up by Griffin et al. (2003)
7c	$\rho_{0.66}/\rho_{1.65}<5.4$	Unclassified	Cloud not picked up by Griffin et al. (2003)
7d	$\rho_{0.66}/\rho_{0.86}>1.2$	Ice	Remaining pixels from step 7 are classified as snow
8	NDSI<0.56 and $\rho_{0.56}/\rho_{0.66}<1.064$	Unclassified	Cloud not picked up by Griffin et al. (2003)
9	NDSI<0.47 and $\rho_{0.56}/\rho_{0.66}>1.76$	Water	
10	$\rho_{0.43}/\rho_{0.56}<1.37$		
10a	$\rho_{0.86}/\rho_{1.65}>1.4$	Ice	Modified by patch in ASE Release 2 (see text)
10b	$\rho_{0.43}/\rho_{0.86}>2.65$	Water	Remaining pixels from step 10 are left as unclassified (clouds not picked up by Griffin et al. (2003))
11	NDSI<0.27	Cloud	
12	$(\rho_{0.86}-\rho_{1.65})/(\rho_{0.86}+\rho_{1.65})>0.71$	Unclassified	Cloud not picked up by Griffin et al. (2003), and shadow
13	$\rho_{0.56}/\rho_{0.66}>1.376$	Water	
14	$\rho_{0.43}/\rho_{0.56}>1.73$	Unclassified	Shadows, all remaining pixels are classified as water

Figure 3: Cryosphere Snow Water Ice Land (SWIL) manually derived classification algorithm (courtesy [Doggett et al. 2006]).

3.2. Flood Classification

The onboard flood classification algorithm is intended to enable onboard recognition of major flooding events [Ip et al. 2006]. Through iterative analysis of data from test sites two algorithms were developed for a range of sediment loads. The first of these flood detection algorithms uses the ratio of 0.55 μm / 0.86 μm Hyperion data. The second utilizes the ratio between the 0.99 μm / 0.86 μm data. One complication in utilizing the flood classifier is accurate estimation of cloud cover for masking the flood scene. In order to address this issue prior to flood detection the images are screened for clouds using a cloud classifier developed by MIT Lincoln Laboratory [Griffin et al. 2003]. Figure 2 shows a sequence of Hyperion flood scenes with the corresponding derived classification maps.

3.3. Cryosphere Classification

EO-1 and ASE also demonstrated onboard classification of Snow, Water, Ice, and Land (SWIL). A classifier was manually derived [Doggett et al. 2006] and later a Support Vector Machine (SVM) algorithms was automatically learned by training on expert labeled data. The manual algorithm is shown below - Figure 3 shows the details of the manual algorithm, and Figure 4 shows a sequence of Hyperion images and derived classification. The cryosphere algorithm uses the Normalized Snow Difference Index (NSDI) defined as:

NSDI =
(0.56μm – 1.65μm)/(0.56μm+1.65μm).

Another cryosphere classifier was developed using Support Vector Machine (SVM) learning techniques and is described in [Castano et al. 2006]. Support vector machine

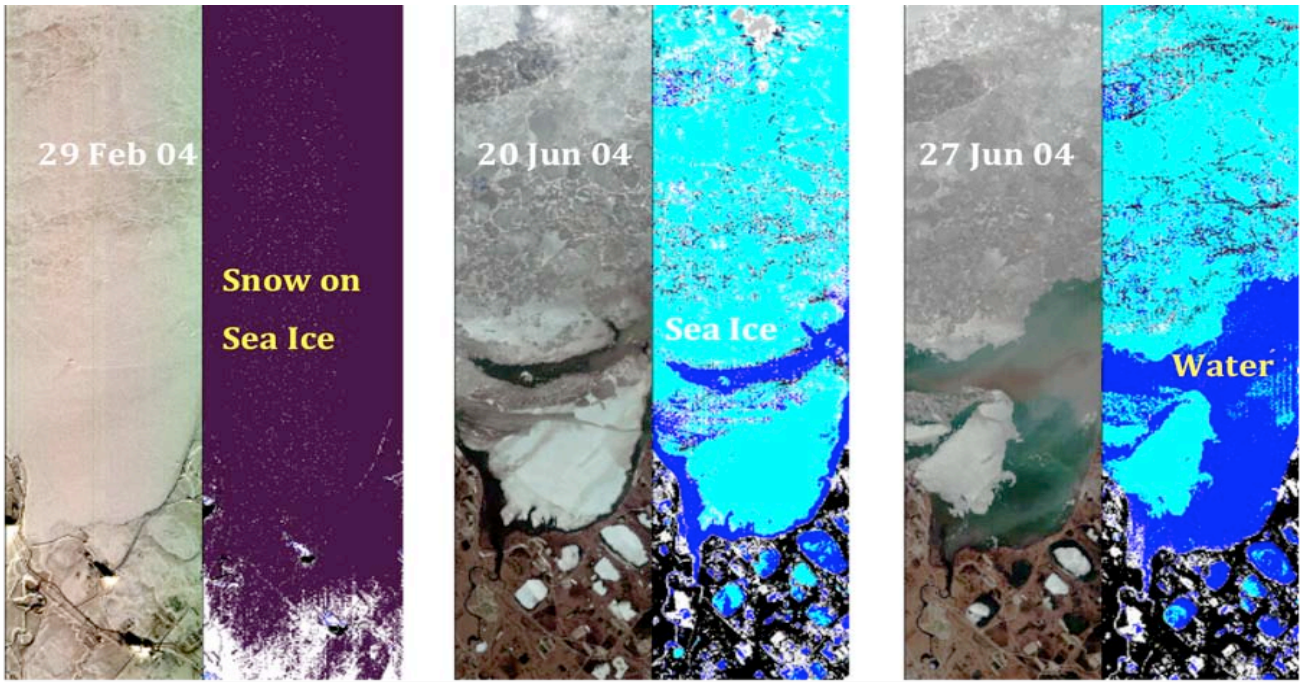

Figure 4: Sequence of false color and classified images as developed onboard EO-1 tracking sea ice breakup at Prudhoe Bay, Alaska, 29 February 2004 – 27 June 2004.

learning techniques automatically derive decision classifiers via mathematical analysis of differences between labelled class examples in input data.

3.4. Onboard Quicklook Processing

Within ASE we have also developed a quicklook image product. For this product an ICER [Kiely and Klimesh 2003] compression of 1 band from onboard science processing (e.g. one of the algorithms above) is compressed into a 20 Kbyte image and downlinked in the engineering S-band channel. Below figure 1B shows a quicklook image of the Mount Saint Helens Volcano taken as part of monitoring image sequence.

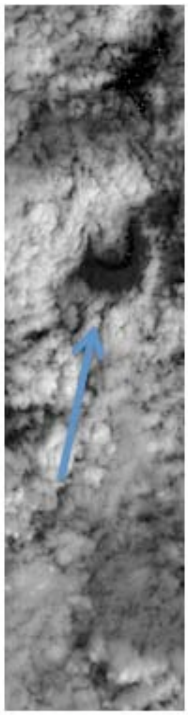

Figure 1B: Quicklook image of Mount Saint Helens (indicated by arrow) using Band 100, 1245 nm compressed using the ICER algorithm for rapid delivery.

4. WORK IN PROGRESS

Ongoing work includes development of products for marine applications and benchmarking algorithms on current and future flight processors to understand onboard processing options for future missions.

4.1. Marine Applications

Ongoing work includes development of rapid products for a range of marine applications. Ground-based processing of marine data for an October 2008 experiment in Monterey Bay [Chien et al. 2009] included acquisition of Hyperion data and delivery of with two derivative science products Fluorescence Line Height (FLH) and Maximum Chlorophyll Index (MCI) linear baseline data products [Gower and Borstad 2004, Gower et al. 2005].

For Hyperion data the FLH and MCI measures were adapted from MODIS definitions:

FLH = (681μm – 660μm)
– 0.4 * (711μm – 660 μm) and
MCI = (711μm – 681μm)
– 0.422 * (752 μm – 660 μm).

Figure 5 shows a sample MCI product produced as part of the October 2008 deployment. Development of FLH and MCI products onboard would enable more rapid dissemination of science results for quick response activities (such as issuing alerts or deployment of sensors for further acquisitions).

4.2. Onboard Processing for Hyspiri

The HyspIRI mission [Green et al. 2008] is a future mission under study by NASA with a visible/hyperspectral (380 nm to 2500 nm, 60m/pixel, 144km swath) and thermal infra-red imaging capability (400nm, 7 bands between 7500 and 1200 nm, 60m/pixel, 600km swath).

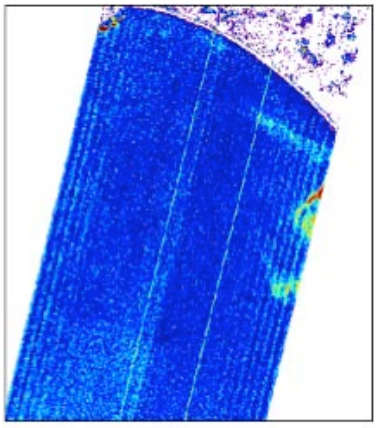

Figure 5: False color Maximum Chlorophyll Index derived from Hyperion imagery of Monterey Bay acquired 21 October 2008. (courtesy MBARI)

NASA is studying an option of use of a hybrid direct broadcast capability to enable rapid delivery of science products. Direct broadcast [Direct Broadcast] transmits instrument data for downlink as it is being acquired so that regional ground stations can receive it in near real time for rapid development of science products. However the amount of data collected by Hyspiri (1 Gbit per second) exceeds the direct broadcast downlink capacity (15 Mbits per second) by approximately 65x. As a result, NASA is studying options to perform onboard processing to develop science products onboard for downlink as the science products are much smaller in size than the complete raw data. While the entire acquired dataset will still be downlinked using polar ground stations (e.g. not in near real time) the direct broadcast product will be available with much shorter latency (within hours from acquisition). An additional problem is that without global direct broadcast coverage (such as over ocean areas) the near real-time data capability is lost. In order to avoid this problem high priority data can be stored onboard and repeated in the direct broadcast channel to guarantee its receipt at a direct broadcast station (at an increased downlink cost from repetition).

As part of this effort, a range of science algorithms using visible, hyperspectral (vnir and swir), and thermal infra-red are being studied for onboard product generation. Directly applicable are many algorithms derived for use with current multispectral and hyperspectral instruments such as MODIS, ASTER, ALI, and Hyperion (see Table below).

Instrument	Spectral Resolution	Spatial Resolution	Instrument Swath
MODIS (Terra, Aqua)	36 bands 405nm-14300 nm	250-1000m	2700 km
ASTER (Terra)	14 bands 520nm-11650nm	30m	60km
ALI, (EO-1)	8 bands 400-2500 nm	30m	28km
Hyperion (EO-1)	8 bands 400-2500 nm	30m	7km
VSWIR, (Hyspiri)	212 bands 380-2500nm	60m	150km
TIR (Hyspiri)	8 bands 400nm 8000-12000 nm	60m	600km

Volcano Monitoring – Volcanic activity can be monitored via analysis of the thermal signature as already demonstrated on EO-1. In these cases detection of a significant thermal signature would trigger sending down any available VSWIR (if covered) else all TIR bands. Hyspiri TIR bands also facilitate tracking of Ash and SO2 plumes that requires sensitivity in the TIR range of 8-10 microns.

Surface water coverage – Flooding can be tracked using VSWIR and TIR instruments. In addition to the algorithms described above there are several MODIS-based algorithms [Sohlberg, Brackenridge] being evaluated.

Cryospheric change – The SWIL algorithm described earlier as well as adaptations of MODIS products for snow coverage [MODIS Sea Ice]. Of particular interest within the cryosphere discipline are rapid response Arctic sea ice products to be used for maritime applications.

Vegetation – another area of interest is tracking of vegetation and plant health using hyperspectral imagery. These use measures such as the Normalized Difference Vegetation Index (NDVI), NGDVI, canopy foliar indices, and other related indices. These products use spectral information in the 550-1640 nm range.

Dust storm tracking – large-scale dust storms [Miller 2003] have also been detected using MODIS and therefore are good candidates for Hyspiri VSWIR and TIR products.

Oceanographic applications – in addition to the ocean biology applications described above we are also assessing possible Sea Surface Temperature (SST) products using the TIR instrument. Prior work has derived SST products from MODIS data [MODIS SST].

In addition to application of the above algorithms we are investigating the use of support vector machine learning techniques to consolidate processing for correction and classification/product generation. In this approach data is corrected and conventional classifications are generated. These are used as labels to a supervised learning algorithms that is trained on uncorrected data. This transfer learning method automatically derives processing that does not rely on corrected data, removing the need for onboard correction. Can use SVM regression methods for indices (e.g. not classes).

These studies include testing the above algorithms on a range of flight processors including the Mongoose M5 (currently flying on EO-1), Atmel (100MHz), Rad 750 (200MHz), as well as more powerful FPGA based Opera, SpaceCube, and Isaac platforms which offer up to 50 GFlops performance. Currently onboard EO-1 running on the M5 processor, the thermal algorithm takes 5 minutes, cloud takes 5-10, SWIL 40-50 minutes, and flood 30-40 minutes onboard EO-1 running on the M5 (with onboard science processing getting ~ 40% of the CPU due to other FSW). In comparison Hyspri is expected to produce approximately 1Gbps raw instrument data and requires approximately 300K pixels processed each second for VSWIR and 1.2M pixels processed each second for TIR in order to keep up with data production.

5. RELATED WORK AND CONCLUSIONS

Other work has studied the use of Support Vector Machine (SVM) learning techniques to onboard detection of active sulfur springs [Mandrake et al, 2009]. This work includes analysis of linear, polynomial, and gaussian kernel SVM's to detection of sulfur in Hyperion images – a very challenging task due to the slight sulfur signature (sub pixel) and limited onboard computing on EO-1. Onboard data analysis algorithms have also been developed for the THEMIS instrument onboard Mars Odyssey [Castano et al. 2007] but as of yet have not been integrated with the flight software or uploaded and used. The Mars Exploration Rovers now have the ability to analyze onboard imagery to detect dust devils and clouds [Castano et al. 2008, Chien

et al. 2008] and a further upload is under way to enable autonomous targeting of remote science instruments onboard MER [Estlin et al. 2009].

We have described a number of algorithms intended for classification of hyperspectral images onboard spacecraft. The thermal event detection and summarization, surface water/flood detection, and snow/water/ice/land cryosphere tracking have been operational onboard the EO-1 spacecraft processing Hyperion data since 2004. We then described ongoing work towards onboard algorithms including marine science products. Onboard production of these science products enables: (1) more rapid delivery of science products and (2) more rapid response to acquire further imagery, issue alerts, or other actions.

REFERENCES

R. Brackenridge and E. Anderson, "MODIS-based flood detection, mapping and measurement: the potential for operational hydrological applications, in Transboundary floods: reducing risks through flood management, Springer 2006.

A. Castano, A. Fukunaga, J. Biesiadecki, L. Neakrase, P. Whelley, R. Greeley, M. Lemmon, R. Castano, S. Chien, "Automatic detection of dust devils and clouds at Mars," Machine Vision & Applications, Oct 2008, vol. 19, No. 5-6, pp. 467-482.

R. Castano, D. Mazzoni, N. Tang, T. Doggett, S. Chien, R. Greeley, B. Cichy, and A. Davies. Onboard classifiers for science event detection on a remote sensing spacecraft. In Proc 12th Intl Conf on Knowledge Discovery & Data Mining, pp 845–851, 2006.

R. Castano, K. Wagstaff, S. Chien, T. Stough, B. Tang, Onboard analysis of uncalibrated data for a spacecraft at Mars, Proceedings 13th International Conference on Knowledge Discovery and Data Mining, August 2007, San Jose, CA.

S. Chien, R. Sherwood, D. Tran, B. Cichy, G. Rabideau, R. Castano, A. Davies, D. Mandl, S. Frye, B. Trout, S. Shulman, D. Boyer, "Using Autonomy Flight Software to Improve Science Return on Earth Observing One, Journal Aerospace Computing, Information, & Comm, April 2005, AIAA.

S. Chien, R. Castano, B. Bornstein, A. Fukunaga, A. Castano, J. Biesiadecki, R. Greeley, P. Whelley, and M. Lemmon, Results from Automated Cloud and Dust Devil Detection Onboard the MER rovers, Intl Symp on Artificial Intelligence, Robotics, & Automation in Space, Universal City, CA, February 2008.

A. G. Davies, S. Chien, V. Baker, T. Doggett, J. Dohm, R. Greeley, F. Ip, R. Castano, B. Cichy, R. Lee, G. Rabideau, D. Tran and R. Sherwood (2006) Monitoring Active Volcanism with the Autonomous Sciencecraft Experiment (ASE). Remote Sensing of Environment, Vol. 101, Issue 4, pp. 427-446.

NASA Direct Broadcast System web page. http://directreadout.sci.gsfc.nasa.gov/

T. Doggett, R. Greeley, A. G. Davies, S. Chien, B. Cichy, R. Castano, K. Williams, V. Baker, J. Dohm and F. Ip (2006) Autonomous On-Board Detection of Cryospheric Change. Remote Sensing of Environment, Vol. 101, Issue 4, pp. 447-462.

T. Estlin, R. Castano, B. Bornstein, D. Gaines, R. C. Anderson, C. de Granville, D. Thompson, M. Burl, S. Chien, and M. Judd, "Automated targeting for the MER rovers." AIAA Infotech @ Aerospace Conference, Seattle, WA, April 2009.

J.F.R. Gower & Borstad, G.A. (2004).On the Potential of Modis and Meris for Imaging Chlorophyll Fluorescence From Space. Intl Journal of Remote Sensing. 25(7-8),1459-1464.

J. Gower, King, S. & Borstad, G., et al. (2005).Detection of Intense Plankton Blooms Using the 709nm Band of the Meris Imaging Spectrometer. Intl Jnl Remote Sensing. 26(9), 2005-2012.

R. Green, G. P. Asner, S. Ungar, R. Knox, "Results of the Decadal Survey Hypsiri Imaging Spectrometer Concept Study: a high signal to noise ratio and high uniformity global mission to measure plant physiology and functional type," Proc IEEE Intl Geoscience & Remote Sensing Symp, Boston, MA, July 2008.

M. K. Griffin, Burke, H. K., Mandl D., & Miller, J., Cloud Cover Detection Algorithm for EO-1 Hyperion Imagery. 17th SPIE AeroSense 2003, Orlando FL, Conf Algorithms & Techno for Multispectral, Hyperspectral and Ultraspectral Imagery IX.

F. Ip, J. M. Dohm, V. R. Baker, T. Doggett, A. G. Davies, R. Castano, S. Chien, B. Cichy, R. Greeley, and R. Sherwood (2006) Development and Testing of the Autonomous Spacecraft Experiment (ASE) floodwater classifiers: Real-time Smart Reconnaissance of Transient Flooding. Remote Sensing of Environment, Vol. 101, Issue 4, pp. 463-481.

A. Kiely and M. Klimesh. The ICER progressive wavelet image compressor. The Interplanetary Network Progress Report, 42155, 2003.

L. Mandrake, K. L. Wagstaff, D. Gleeson, U. Rebbapragada, D. Tran, R. Castano, S. Chien, R. T. Pappalardo, Onboard detection of naturally occurring sulfur on a glacier via an onboard SVM and Hyperion/EO-1, submitted to IEEE Workshop on Hyperspectral Image and Signal Processing: Evolution in Remote Sensing, 2009.

Miller, S. D. (2003), A consolidated technique for enhancing desert dust storms with MODIS, Geophys. Res. Lett., 30(20), 2071, doi:10.1029/2003GL018279.

MODIS sea ice products http://modis-snow-ice.gsfc.nasa.gov/

MODIS sea surface temperature products, http://podaac.jpl.nasa.gov/pub/documents/dataset_docs/modis_sst.html

Rad750, http://www.baesystems.com/ProductsServices/bae_prod_s2_rad750.html

D. Speer, K. Stewart, G. Jackson, A. Hernandez-Pellerano, "The Space Technology 5 Avionics System, " IEEE Aerospace Conference, 2005.

C. J. Tucker (1979). Red and photographic infrared linear combinations for monitoring vegetation. Remote Sensing of Environment, 8, 127−150.

S. G. Ungar et al, "Overview of the Earth Observing One (EO-1) Mission", IEEE Transactions on Geoscience & Remote Sensing, vol. 41, No. 6, June 2003.